**Iranian Journal of Geophysics, Vol 15 No 4, 2022, Page 127 – 137 (Research Article)**
**DOI: 10.30499/IJG.2021.289201.1334**

# Comparison of precise point positioning method using online services and open-source software

Abdolreza Safari[1], Saeed Farzaneh [2*] and Kamal Parvazi[3]

[1] *Professor, School of Surveying and Geospatial Engineering, College of Engineering, University of Tehran, Iran*
[2] *Assistant Professor, School of Surveying and Geospatial Engineering, College of Engineering, University of Tehran, Iran*
[3] *Ph.D. Student of Geodesy, School of Surveying and Geospatial Engineering, College of Engineering University of Tehran, Iran*

(Received: 06 June 2021, Accepted: 02 September 2021)

## Abstract

Since many sophisticated Global Navigation Satellite System (GNSS) applications require satellite precise ephemeris (orbit and clock products), in recent years, many organizations have been responsible to provide users with information on GNSS. With the advent of these products, a positioning method known as Precise Point Positioning (PPP) was introduced. This technique is based on only using the observations of one receiver. Therefore, it is possible to determine the position using the observation of code and phase. In the last decade, due to the advent of this technique, achieving high accuracy, the need of only one receiver instead of differential observations, as well as reducing the cost of operation is possible by users for scientific and commercial research. This technique makes it possible to determine the position with a precision of centimetres to decimetres for static and kinematic applications. According to the results presented in the review of two case studies, comparison of estimated results with the actual values provides centimeters-level accuracy. For this reason, these services can be used to access the position components using PPP. In this research, the accuracy of the PPP method has been evaluated. The observations of four stations have been used globally. The collected data is processed using online services and open source software. Finally, the relevant results have been carefully examined. Based on the results presented in the first part and comparison with the final characteristics of the known points in the study area, on average, a difference of 3 mm has been reported when using 24 hours of observation. Considering the set of observations related to ten points in six-time intervals, the accuracies provided for the X, Y and Z coordinate components in the first period are 42, 31 and 20 mm, respectively and in the sixth period, the values of 9, 11 and 7 mm are reported.

**Keywords:** Precise Point Positioning (PPP), PPP Online Service, Global Navigation Satellite System (GNSS), open-source software

## 1 Introduction

With upgrading and development of the GPS, reusing the Russian GLONASS satellites, and setting up most of Europe's Galileo satellite navigation system, it became possible to receive information from more satellites. (Ogutcu, 2020; Falcone, 2016; Alkan et al., 2017). The number of GNSS frequencies and satellites is constantly increasing. The basic idea of all satellite positioning systems is the same. However, these systems differ in many aspects now. One of them is the difference in the used coordinate frames. In order to apply multi-system observations and frequencies, calibration parameters must be specified for them and made available to users (Dalla Torre and Caporali, 2015). Accordingly, the International GNSS Service (IGS) makes Multi-GNSS Observation and Analysis Services available to the public (Montenbruck et al., 2014). The MGEX analysis center now provides productions of satellite clock and orbit precise correction for all systems as well as satellite phase center offset information and biases related to code and phase (Montenbruck et al., 2017; Bahadur and Nohutcu, 2019).

PPP can reach an accuracy of centimeter using accurate satellite clock and orbit information and ionospheric-free observations, as well as applying corrections to observations such as phase deflection error correction, satellite and receiver antenna phase center separation, relativity effect, effects of station displacement due to oceanic loading and solid earth tide, Earth's rotation parameters changes, etc. (Jan and Pierre, 2001; Bisnath and Gao, 2009). However, to achieve coordinate components with centimeter-level accuracy, the PPP method typically needs about 30 minutes. PPP convergence is defined as the accuracy estimation for position components (two-dimensional or three-dimensional position) consistently reaching a certain level of accuracy (e.g., centimeter accuracy level). This means that the method can keep the accuracy of the horizontal or vertical component at the level of centimeter accuracy at a 95% confidence level. In other words, the floating phase ambiguity continuously reaches constant values and then does not leave these values. In general, convergence in PPP depends on characteristics such as (1) the number of satellites and their geometry, (2) the dynamics and environment of the receiver, and (3) the quality of the observation and sampling interval. Therefore, in PPP mode, long time required for convergence is a challenging issue (Bisnath and Gao, 2009). Positioning accuracy and time required for convergence in PPP mode depend on the number and geometry of satellites, the quality of the pseudo-range-code observations, applying the correct weight of the observations (presenting a suitable stochastic model), unity of the phase observations, and the measurement rate (Bisnath and Gao, 2009). To reduce convergence time, one of the ideas used is to increase the degree of freedom using combination of GNSS observations. Today, owing to the existence of GLONASS and developments of other global navigation systems such as Galileo and BeiDou, the combination of observations of these systems to increase the degree of freedom of the system of observation equations and help to increase the speed of convergence and improve accuracy are proposed as alternative solutions in precise point positioning (Afifi and El-Rabbany, 2014; Cao et al., 2010; Li and Zhang, 2014).

In this study, to evaluate the PPP method in static mode, an experiment was performed in different modes. Therefore, observations in the static mode were processed using scientific/commercial software, OPUS, APPS, CSRS-PPP, GAPS, AUSPOS, and gLAB. The experiment was performed in two cases. In the first case, considering the stations that exist in the IGS international network, the processing was performed using each of the mentioned systems and software. In this case, the estimated coordinates, as well as the accuracy obtained for the coordinates were compared with the coordinates and the final accuracy provided by IGS for each station. The stations used had observations with a sampling interval of 30 seconds. These stations were selected in different parts of the world. In the next stage, by considering stations in the region of Iran and applying this strategy, the positioning is done in periods of 4, 8, 12, 16, 20 and 24 hours. At this stage, coordinate and accuracy observations were estimated for each period. Furthermore, the effect of observation harvest time on presentation accuracy by PPP method was investigated. The results are compared with the final output provided by IGS. In the following, the results of this experiment are presented.

## 2 Functional models for Multi-GNSS Precise Point Positioning technique

Due to the many applications of navigation systems in research studies as well as the effect of environmental conditions on observations, various models have been proposed to reduce systematic errors. Today, the use of a combination of GNSS observations is proposed as one of the conventional models. In the case of a combination of observations, the simplest way is to use satellite and orbit satellites in the same coordinate system. This mode is used to improve the accuracy of observations in the PPP positioning method. In this case, to remove the ionosphere error effect, an ionospheric-free model is used for code and phase observations. On the other hand, it is possible to eliminate the satellite clock error by using precise ephemeris. With the help of existing models, it is also possible to eliminate or reduce errors such as phase center offset satellite and receiver, tides, and relativity (Bisnath and Gao, 2009; Paziewski et al., 2018). In addition, other sources of error such as the troposphere effect as well as the receiver clock error are estimated along with other model unknowns. Therefore, the ionospheric-free functional model for observations in PPP positioning is as follows:

$$\begin{cases} \begin{cases} P_{IF,r}^{s,j} = \rho_r^{s,j} + c\tilde{dt}_r^s - c\tilde{dT}^{s,j} + T_r^{s,j} + \varepsilon(P_{IF,r}^{s,j}) \\ L_{IF,r}^{s,j} = \rho_r^{s,j} + c\tilde{dt}_r^s - c\tilde{dT}^{s,j} + T_r^{s,j} + \lambda_{IF}^{s,j}\tilde{N}_{IF}^{s,j} + \varepsilon(L_{IF,r}^{s,j}) \end{cases} \\ \begin{cases} c\tilde{dt}_r^s = cdt_r^s + b_{IF,r}^s \\ c\tilde{dT}^{s,j} = cdT^{s,j} + b_{IF}^{s,j} \\ \tilde{N}_{IF}^{s,j} = N_{IF}^{s,j} + (B_{IF,r}^s - b_{IF,r}^s) - (B_{IF}^{s,j} - b_{IF}^{s,j}) \end{cases} \end{cases} \quad (1)$$

In Equation (2), $\rho_r^{s,j}$ geometric distance between receiver, $c$ speed of light, $c\tilde{dt}_r^s$ receiver clock errors, $c\tilde{dT}^{s,j}$ satellite clock errors, $T_r^{s,j}$ Tropospheric delay parameter, $\varepsilon$ Observation noise parameter, $\lambda_{IF}^s$ wavelengths ( $L_1$ and $L_2$ ), $\tilde{N}_{IF}^{s,j}$ phase ambiguity, $b_{IF,r}^s$ receiver code hardware bias, $B_{IF,r}^s$ receiver phase hardware bias, $b_{IF}^{s,j}$ satellite code hardware bias, $B_{IF}^{s,j}$ satellite phase hardware bias, $s$ type of satellite system, and $j$ satellite number, respectively. In Equation (2), G, R, and E are used for GPS, GLONASS, and Galileo systems, respectively. Finally, After the introduction of the new parameter, the time difference between the systems as well as the combination of different observations, the observation equations are presented as follows:

$$\begin{cases} \begin{cases} P_{IF,r}^{G,j} = \rho_r^{G,j} + c\tilde{dt}_r^G + T_r^{G,j} + \varepsilon(P_{IF,r}^{G,j}) \\ L_{IF,r}^{G,j} = \rho_r^{G,j} + c\tilde{dt}_r^G + T_r^{E,j} + \lambda_{IF}^G\tilde{N}_{IF}^{G,j} + \varepsilon(L_{IF,r}^{G,j}) \end{cases} \\ \begin{cases} P_{IF,r}^{R,j} = \rho_r^{R,j} + c\tilde{dt}_r^G + cdt_{sys}^R + T_r^{R,j} + \varepsilon(P_{IF,r}^{R,j}) \\ L_{IF,r}^{R,j} = \rho_r^{R,j} + c\tilde{dt}_r^G + cdt_{sys}^R + T_r^{R,j} + \lambda_{IF}^R\tilde{N}_{IF}^{R,j} + \varepsilon(L_{IF,r}^{R,j}) \end{cases} \\ \begin{cases} P_{IF,r}^{E,j} = \rho_r^{E,j} + c\tilde{dt}_r^G + cdt_{sys}^E + T_r^{E,j} + \varepsilon(P_{IF,r}^{E,j}) \\ L_{IF,r}^{E,j} = \rho_r^{E,j} + c\tilde{dt}_r^G + cdt_{sys}^E + T_r^{E,j} + \lambda_{IF}^E\tilde{N}_{IF}^{E,j} + \varepsilon(L_{IF,r}^{E,j}) \end{cases} \end{cases} \quad (2)$$

In Equation (2), $cdt_{sys}^E$ and $cdt_{sys}^R$ and represent the time difference between the GPS system and the Galileo and GLONASS systems.

## 3 Processing GNSS observations using online services and software

For processing GNSS observations, there are now many online services and software freely available to users. Different organizations present different services. Therefore, their processing methods, processing options, and output format are different. Some of these services and software are OPUS, APPS, CSRS-PPP, GAPS, AUSPOS and gLAB. In CSRS-PPP system, the estimated positions for the points are presented relative to base level NAD83. This service allows the use of single and dual-frequency observations of both GPS and GLONASS systems (Mendez Astudillo et al., 2018). The GAPS service was developed by UNB (Albayrak et al., 2020). APPS was presented by JPL. In the latter system, positioning is performed based on GIPSY-OASIS software (Albayrak et al., 2020). AUSPOS is a precise point positioning online service developed in Australia (Albayrak et al., 2020) and OPUS was developed by NOAA (Xu et al., 2020). gLAB is a develop-based software of European Space Agency (ESA) via a contract by the Astronomy and Geomatics Research Group (gAGE) of the Politecnica de Catalunya (UPC). This software is a multi-purpose educational package for processing and analyzing GNSS data (Mendez Astudillo et al., 2018). The quality of presented processing results depends on the availability, proximity, and quality of the reference station data and the availability of the precise orbit and clock of satellite. Table 1 presents detailed specifications of each system.

**Table 1.** Processing settings for PPP online services and software.

| PPP Service | gLAB | GAPS | CSRS-PPP | APPS | OPUS | AUSPOS |
|---|---|---|---|---|---|---|
| GNSS system(s) | GPS only | GPS, Galileo and BeiDou | GPS and GLONASS | GPS only | GPS only | GPS only |
| Modeled observable | Dual-frequency | Undifferenced, ionosphere-free linear combination | Dual-frequency | Dual-frequency | ionosphere-free linear combination | Double differences of the ionosphere-free linear combination |
| Organizations | European Space Agency (ESA) | University of New Brunswick | National Resources Canada (NRCan) | Jet Propulsion Laboratory (JPL) | NOAA National Geodetic Survey (NGS) | Geoscience Australia |
| Website | https://gage.upc.edu/ | http://gaps.gge.unb.ca/submitbasic.php | https://webapp.geod.nrcan.gc.ca/geod/tools-outils/ppp.php | https://apps.gdgps.net/apps_file_upload.php | https://www.ngs.noaa.gov/OPUS/ | https://gnss.ga.gov.au/auspos |

## 4 Experiment design, results and discussions

A suitable data source for multi-GNSS PPP positioning is the use of the multi-GNSS experiment (MGEX), whose stations are evenly distributed all over the world and can track most navigation satellite systems. Data were collected from four MGEX stations with global distribution. The stations used can track the satellites of all four systems. The observation time for each station is 24 hours and the sampling interval is 30 seconds. These observations were collected over a period of one week. Fig. 1 shows the location of these stations.

In the following, the observations related to four stations are processed by the services presented in Table 2, and using PPP method. The results related to analyzing GPS, GPS/GLONASS and Multi-GNSS observations are presented in Tables 2 and 3, respectively.

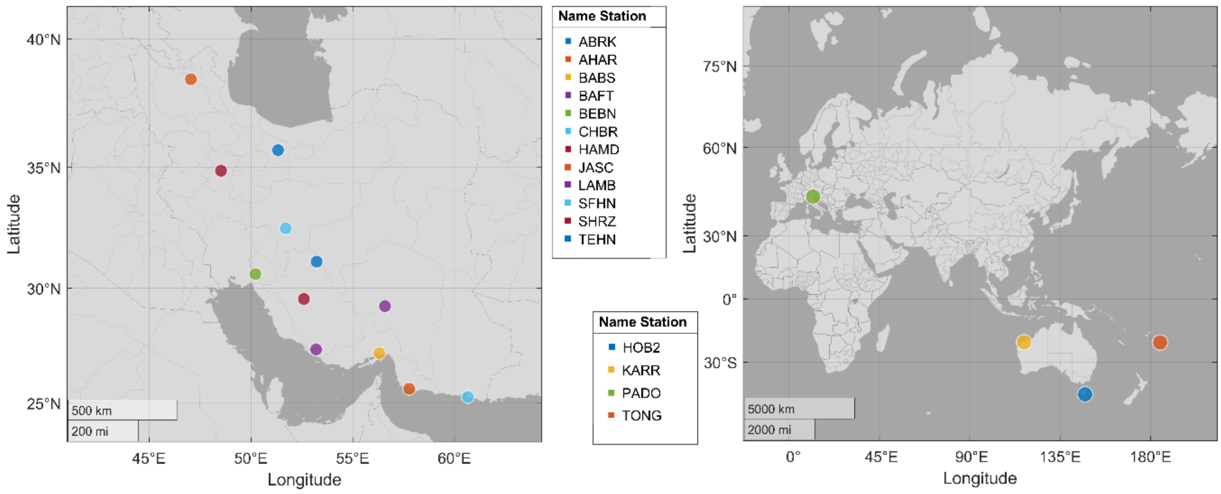


**Fig 1.** Distribution of the four MGEX stations.

**Table 2.** Comparison of the results obtained from IGS and gLAB online services using GPS observations.

| Station / Solution | | PADO | HOB2 | KARR | TONG |
|---|---|---|---|---|---|
| Final_IGS | X | 4388881.793±0.0013 | -3950072.188 ± 0.0008 | -2713833.199±0.0007 | -5930303.535±0.0016 |
| | Y | 924567.700 ± 0.0006 | 2522415.356 ± 0.0006 | 5303935.109 ± 0.0011 | -500148.590 ± 0.0005 |
| | Z | 4519588.874 ± 0.0014 | -4311637.481 ± 0.0008 | -2269513.844±0.0006 | -2286366.266 ±0.0007 |
| gLAB | X | 4388881.797 ± 0.0090 | -3950072.194 ± 0.0086 | -2713833.199±0.0084 | -5930303.539 ±0.0130 |
| | Y | 924567.701 ± 0.0062 | 2522415.366 ± 0.0070 | 5303935.103 ± 0.0122 | -500148.593 ± 0.0071 |
| | Z | 4519588.871 ± 0.0087 | -4311637.493 ± 0.0082 | -2269513.842±0.0054 | -2286366.273 ±0.0057 |
| APPS | X | 4388881.794 ± 0.0013 | -3950072.192 ± 0.0012 | -2713833.200±0.0010 | -5930303.542 ±0.0020 |
| | Y | 924567.701 ± 0.0005 | 2522415.357 ± 0.0008 | 5303935.110 ± 0.0017 | -500148.591 ± 0.0006 |
| | Z | 4519588.875 ± 0.0013 | -4311637.482 ± 0.0013 | -2269513.843±0.0008 | -2286366.270 ±0.0009 |
| GAPS | X | 4388881.796 ± 0.0017 | -3950072.186 ± 0.0015 | -2713833.198±0.0015 | -5930303.530 ±0.0024 |
| | Y | 924567.707 ± 0.0012 | 2522415.350 ± 0.0013 | 5303935.104 ± 0.0022 | -500148.594 ± 0.0013 |
| | Z | 4519588.886 ± 0.0016 | -4311637.490 ± 0.0015 | -2269513.848±0.0010 | -2286366.272 ±0.0010 |
| OPUS | X | 4388881.799 ± 0.016 | -3950072.186 ± 0.007 | -2713833.203 ± 0.013 | -5930303.527 ± 0.023 |
| | Y | 924567.701 ± 0.008 | 2522415.353 ± 0.003 | 5303935.110 ± 0.013 | -500148.593 ± 0.004 |
| | Z | 4519588.876 ± 0.006 | -4311637.479 ± 0.008 | -2269513.842 ± 0.004 | -2286366.267 ± 0.009 |
| AUSPOS | X | 4388881.792 ± 0.003 | -3950072.189 ± 0.004 | -2713833.198 ± 0.003 | -5930303.535 ± 0.006 |
| | Y | 924567.700 ± 0.003 | 2522415.357 ± 0.004 | 5303935.104 ± 0.003 | -500148.588 ± 0.004 |
| | Z | 4519588.875 ± 0.007 | -4311637.482 ± 0.008 | -2269513.842 ± 0.007 | -2286366.270 ± 0.011 |

**Table 3.** Comparison of results obtained from IGS, CSRS-PPP using GPS and GLONASS observations.

| Station / Solution | | PADO | HOB2 | KARR | TONG |
|---|---|---|---|---|---|
| Final IGS | X | 4388881.793±0.0013 | -3950072.188±0.0008 | -2713833.199±0.0007 | -5930303.535±0.0016 |
| | Y | 924567.700 ± 0.0006 | 2522415.356±0.0006 | 5303935.109±0.0011 | -500148.590 ±0.0005 |
| | Z | 4519588.874±0.0014 | -4311637.481±0.0008 | -2269513.844±0.0006 | -2286366.266±0.0007 |
| | | | | | |
| CSRS-PPP | X | 4388881.794±0.0053 | -3950072.188±0.0048 | -2713833.197±0.0039 | -5930303.536±0.0080 |
| | Y | 924567.700 ± 0.0023 | 2522415.354±0.0035 | 5303935.105±0.0069 | -500148.590 ±0.0023 |
| | Z | 4519588.873±0.0054 | -4311637.482±0.0050 | -2269513.843±0.0035 | -2286366.267±0.0036 |

Based on the results presented in Tables 2 and 3 and considering the coordinates estimated by the online services and the mentioned software, there is a slight difference in the three components (X, Y, Z) with the final IGS coordinates. The difference in the presented results is due to the use of different processing methods as well as the weighting model of which each system uses. One of the reasons for the difference in presented results can be the effect of the different weight matrices used for code and phase observations during processing. This can also be seen in the combination of different satellite positioning systems. Adding observations of other systems to the GPS does not necessarily lead to better results. However, this goal can be achieved if for each system we use a realistic weight matrix related to its observations for processing.

Then, considering the stations in Iran whose information is available in the IGS international service, the necessary processing has been done by these services. These processes were performed in two modes. The first case is the online services that made it possible to process the required observation files by uploading and sending the necessary outputs. Details of these online services are also provided in Table 1. In the second case, the results were presented with the help of a set of software's that is available to users for free and non-commercially and is used for various applications today. In the Iran region, there are two permanent international stations called TEHN in Tehran and HAMD in Hamedan. Information about these two stations is presented in Table 4. The results related to the processing of these two stations using different services are presented in Table 5.

**Table 4.** Details of stations used in Iran (longitude and latitude per unit degree and height per meter).

| Station | Description | Antenna | Receiver | Lat. | Lon. | Height |
|---|---|---|---|---|---|---|
| HAMD | Hamedan, IRAN | TRM57971.00 SCIT | TRIMBLE NETR9 | 34.868 | 48.534 | 1751 |
| TEHN | Tehran, IRAN | TRM57971.00 NONE | TRIMBLE NETR9 | 35.697 | 51.334 | 1194.6 |

**Table 5.** Comparison of results obtained from IGS, gLAB and online services.

| Station / Solution | | HAMD | TEHN | Station / Solution | | HAMD | TEHN |
|---|---|---|---|---|---|---|---|
| Final_IGS | X | 3469897.619 ± 0.0026 | 3240498.889 ± 0.0013 | gLAB | X | 3469897.570 ± 0.0030 | 3240498.887 ± 0.0038 |
| | Y | 3926741.532 ± 0.0028 | 4049740.451 ± 0.0015 | | Y | 3926741.474 ± 0.0032 | 4049740.448 ± 0.0045 |
| | Z | 3626961.438 ± 0.0025 | 3701663.307 ± 0.0013 | | Z | 3626961.386 ± 0.0027 | 3701663.309 ± 0.0038 |
| CSRS-PPP | X | 3469897.574 ± 0.0054 | 3240498.889 ± 0.0070 | GAPS | X | 3469897.566 ± 0.0015 | 3240498.881 ± 0.0017 |
| | Y | 3926741.480 ± 0.0060 | 4049740.451 ± 0.0083 | | Y | 3926741.473 ± 0.0016 | 4049740.445 ± 0.0020 |
| | Z | 3626961.390 ± 0.0054 | 3701663.308 ± 0.0074 | | Z | 3626961.395 ± 0.0013 | 3701663.316 ± 0.0017 |
| OPUS | X | 3469897.575 ± 0.007 | 3240498.891 ± 0.005 | AUSPOS | X | 3469897.572 ± 0.005 | 3240498.887 ± 0.005 |
| | Y | 3926741.482 ± 0.009 | 4049740.454 ± 0.008 | | Y | 3926741.480 ± 0.003 | 4049740.451 ± 0.003 |
| | Z | 3626961.394 ± 0.008 | 3701663.313 ± 0.006 | | Z | 3626961.388 ± 0.010 | 3701663.308 ± 0.009 |

According to the results of Table 5, using the CSRS-PPP Sigma online service can provide results closer to the actual values. One of the reasons for the higher accuracy of this service is the use of simultaneous observations of GPS and GLONASS and the other is the update of this service last year. Other online services, as well as gLAB software, have provided close results. Among these services, the GAPS service has provided relatively less accurate results than the others. It should be noted that since Hamedan station has been recently added to the IGS international service, its exact location is available in the final coordinate files provided by this center on most days. In the following, considering that the CSRS-PPP service can use the observations of two GPS and GLONASS systems, the component of measuring the duration of observation in ten stations in Iran using this system will be investigated and studied by comparing the accuracy of coordinate components. The system uses GPS and GLONASS observations as well as NRCanPPP software for processing. A standard deviation of 2 meters is also used for code observations, and a 10 mm standard deviation for phase observations. The elevation angle is applied for observations of 7.5 degrees. The Tropospheric Mapping Function used is VMF1_HT (Boehm et al., 2006). Modeling the observable is also performed using dual-frequency observations. Geophysical models are also examined by considering, ocean tide loading, solid earth tides, pole tides and plate tectonic motion (Rizos et al., 2012; Yavaşoğlu et al., 2011). Processing is done statically and kinematically. The tropospheric delay model is applied by two models: Dry delay: Davis and Wet delay: Hopf. Relativistic effects were also applied. In Table 6, information about these stations is provided. 24 hours of observations done with a 30-second interval were divided into 6-time variants (4h, 8h, 12h, 16h, 20h, 24h) and the detected signals (observations at frequencies L1/L2 and signals from the GPS and GLONASS) were selected. The observations of these stations are related to the national network of the National Cartographic Center of Iran. These stations are not part of the IGS network and have been used to discuss coordinate accuracy. In Table 7, the results related to the comparison of the estimated coordinate accuracy in each set of observations are presented. Figs. 2, 3 and 4 show how to improve the accuracy of coordinate components by increasing the observation time.

**Table 6.** Details of stations used in Iran.

| Station | Antenna | Receiver | Date | Station | Antenna | Receiver | Date |
|---|---|---|---|---|---|---|---|
| (SFHN) Isfahan | ASH701945E_M SNOW | ASHTECH UZ-12 | 2011-02-26 | (BABS) Bandar Abbas | ASH701945G_M SNOW | ASHTECH UZ-12 | 2009-01-30 |
| (SHRZ) Shiraz | ASH701945E_M SNOW | ASHTECH UZ-12 | 2010-12-16 | (BEBN) Behbahan | ASH701945E_M SNOW | ASHTECH UZ-12 | 2011-01-04 |
| (ABRK) Abarkooh | ASH701945E_M SNOW | ASHTECH UZ-12 | 2011-01-01 | (CHBR) Chabahar | ASH701945B_M SNOW | ASHTECH UZ-12 | 2009-02-27 |
| (AHAR) Ahar | ASH701945B_M SNOW | ASHTECH UZ-12 | 2012-07-01 | (JASC) Jasc | ASH701945B_M | ASHTECH UZ-12 | 2009-03-02 |
| (BAFT) Baft | ASH701945G_M SNOW | ASHTECH UZ-12 | 2009-02-25 | (LAMD) Lamerd | ASH701945E_M SNOW | ASHTECH UZ-12 | 2011-01-12 |

**Table 7.** Comparison of the estimated coordinate accuracy for each set of observations at each station (units: meters).

| Station | | 4 hours | 8 hours | 12 hours | 16 hours | 20 hours | 24 hours |
|---|---|---|---|---|---|---|---|
| SFHN | X | 0.0320 | 0.0142 | 0.0119 | 0.0108 | 0.0093 | 0.0085 |
| | Y | 0.0231 | 0.0174 | 0.0146 | 0.0118 | 0.0108 | 0.0099 |
| | Z | 0.0196 | 0.0119 | 0.0101 | 0.0085 | 0.0076 | 0.0070 |
| SHRZ | X | 0.0292 | 0.0209 | 0.0132 | 0.0108 | 0.0102 | 0.0093 |
| | Y | 0.0391 | 0.0178 | 0.0140 | 0.0128 | 0.0109 | 0.0102 |
| | Z | 0.0216 | 0.0121 | 0.0092 | 0.0081 | 0.0072 | 0.0066 |
| ABRK | X | 0.0359 | 0.0215 | 0.0123 | 0.0109 | 0.0101 | 0.0088 |
| | Y | 0.0320 | 0.0164 | 0.0141 | 0.0124 | 0.0108 | 0.0100 |
| | Z | 0.0202 | 0.0129 | 0.0097 | 0.0086 | 0.0076 | 0.0068 |
| AHAR | X | 0.0355 | 0.0177 | 0.0120 | 0.0107 | 0.0097 | 0.0082 |
| | Y | 0.0206 | 0.0151 | 0.0127 | 0.0104 | 0.0091 | 0.0086 |
| | Z | 0.0219 | 0.0138 | 0.0107 | 0.0093 | 0.0082 | 0.0074 |
| BAFT | X | 0.0436 | 0.0156 | 0.0116 | 0.0108 | 0.0097 | 0.0084 |
| | Y | 0.0281 | 0.0163 | 0.0147 | 0.0127 | 0.0114 | 0.0104 |
| | Z | 0.0183 | 0.0105 | 0.0090 | 0.0081 | 0.0072 | 0.0065 |
| BABS | X | 0.0533 | 0.0233 | 0.0130 | 0.0116 | 0.0110 | 0.0096 |
| | Y | 0.0378 | 0.0200 | 0.0166 | 0.0149 | 0.0137 | 0.0124 |
| | Z | 0.0241 | 0.0136 | 0.0102 | 0.0092 | 0.0085 | 0.0077 |
| BEBN | X | 0.0370 | 0.0217 | 0.0125 | 0.0113 | 0.0104 | 0.0091 |
| | Y | 0.0281 | 0.0157 | 0.0136 | 0.0121 | 0.0106 | 0.0099 |
| | Z | 0.0180 | 0.0124 | 0.0092 | 0.0083 | 0.0074 | 0.0067 |
| CHBR | X | 0.0450 | 0.0155 | 0.0118 | 0.0110 | 0.0099 | 0.0085 |
| | Y | 0.0349 | 0.0195 | 0.0170 | 0.0148 | 0.0133 | 0.0120 |
| | Z | 0.0179 | 0.0107 | 0.0091 | 0.0082 | 0.0073 | 0.0065 |
| JASC | X | 0.0411 | 0.0151 | 0.0112 | 0.0107 | 0.0100 | 0.0092 |
| | Y | 0.0296 | 0.0170 | 0.0152 | 0.0137 | 0.0123 | 0.0114 |
| | Z | 0.0161 | 0.0096 | 0.0080 | 0.0074 | 0.0068 | 0.0063 |
| LAMD | X | 0.0722 | 0.0340 | 0.0203 | 0.0188 | 0.0170 | 0.0149 |
| | Y | 0.0381 | 0.0262 | 0.0235 | 0.0206 | 0.0189 | 0.0174 |
| | Z | 0.0270 | 0.0162 | 0.0128 | 0.0117 | 0.0106 | 0.0096 |

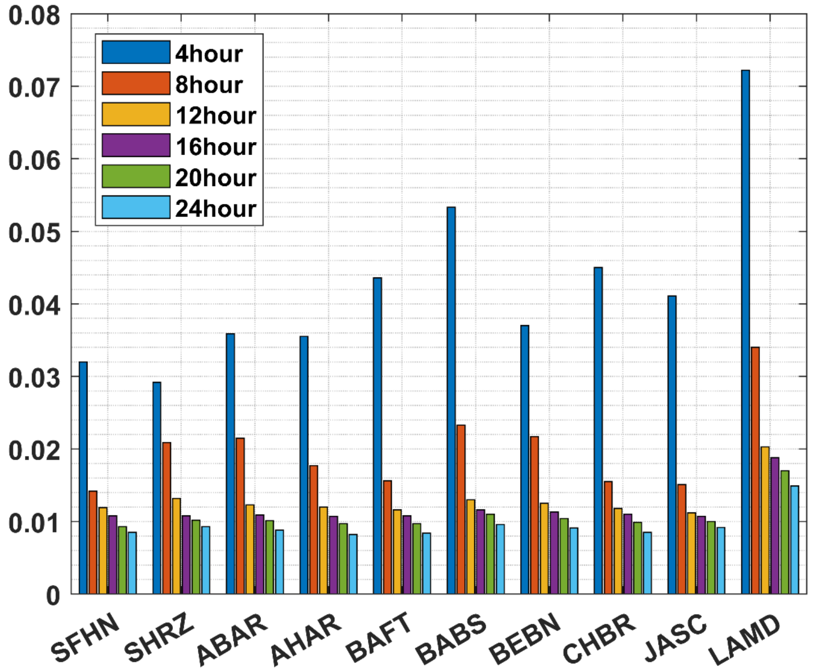


**Fig 2.** The accuracy of X coordinate in time intervals of 4, 8, 12, 16, 20 and 24 hours. The horizontal axis represents each station and the vertical axis expresses the amount of accuracy for the desired component in terms of meters.

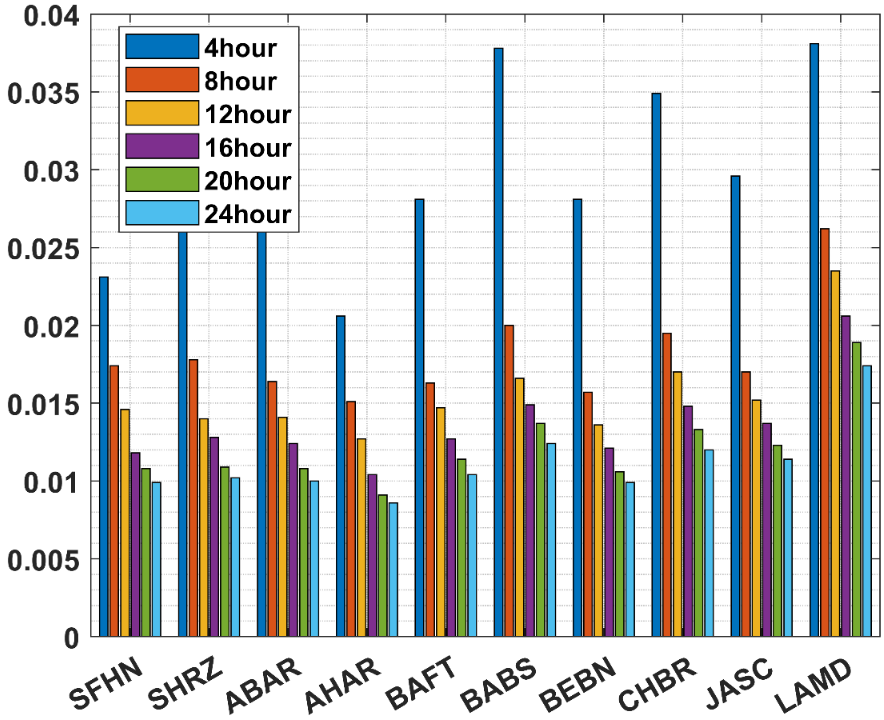


**Fig 3.** The accuracy of Y coordinate in time intervals of 4, 8, 12, 16, 20 and 24 hours. The horizontal axis represents each station and the vertical axis expresses the amount of accuracy for the desired component in terms of meters.

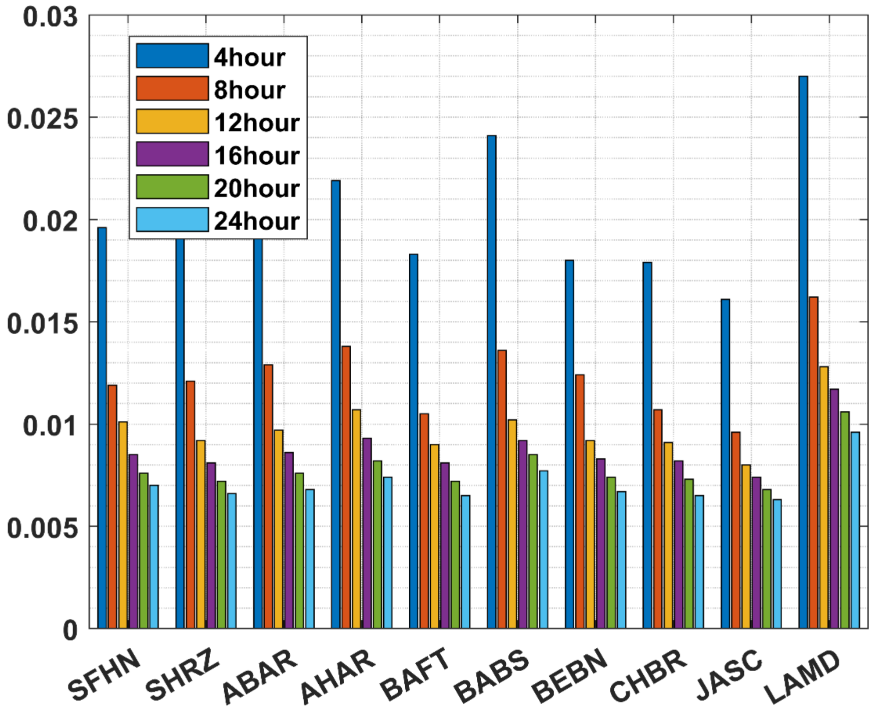


**Fig 4.** The accuracy of Z coordinate in time intervals of 4, 8, 12, 16, 20 and 24 hours. The horizontal axis represents each station and the vertical axis expresses the amount of accuracy for the desired component in terms of meters.

In the PPP method, unknowns include coordinate components, tropospheric delay, phase ambiguity and receiver clock error. To determine the static position in each epoch, these unknowns can be estimated. Accuracy values are considered for the three coordinate components in the last observation epoch. This is possible through the least-squares method and using the accuracy matrix of unknowns. Finally, using the least-squares method, the desired unknowns as well as their accuracy can be estimated. According to the results in Table 7 and Figures 2 to 4, the estimated accuracy for the three coordinate components was performed at ten stations in Iran. This study was performed in six-time intervals of 4, 8, 12, 16, 20 and 24 hours. Accordingly, as can be seen, increasing the observation period leads to improved accuracy in all three components. By comparing the estimated accuracy in ten stations in the shortest period and the maximum time interval, the maximum, minimum and average of this difference for component X are 0.057, 0.02, and 0.033 meters, respectively. The same comparison is provided for the Y component of 0.029, 0.012 and 0.02 meters, respectively. For the Z component, this comparison also shows the numbers 0.017, 0.01 and 0.013 meters. Therefore, it can be concluded that in the PPP method, the period used plays an important role in achieving high accuracy. The observation time parameter can affect the PPP method when the Earth tectonic movement is correctly applied to the coordinates in each observation period. This feature is also available through online services. By choosing the right period, it is possible to improve the quality of the estimated coordinates and their accuracy to be achieved. By using only one receiver in a suitable period and the services mentioned, to achieve a good accuracy is possible.

## 5 Conclusion

In this study, the performance of the method the PPP in static mode using online services as well as open-source software was investigated and analyzed. The results showed that according to the PPP method, with less cost and only using one receiver, the centimeter and decimeter accuracy can be achieved on the coordinates. Based on the accuracy obtained, it can be concluded that the PPP method can be used for surveying applications that require centimeter accuracy. Therefore, when this method is used to determine the position in engineering projects, it is possible for users to perform accurate analysis and achieve high reliability using these services and software. It should also be borne in mind that using the results, if not analyzed, can lead to gross errors. Therefore, based on what was presented, we can say that by performing the desired processes with the existing set of services, we can ensure the accuracy of our results, which is the benefit of using these services.

**Acknowledgments**

The authors thank the IGS system for providing free access to GNSS data. We also thank the online service (APPS, AUSPOS, OPUS, CSRS-PPP, GAPS) that made it possible to process the observations. Finally, thanks to the editor and two anonymous reviewers who helped improve the manuscript.

## References

Afifi, A., and El-Rabbany, A., 2014, Single frequency GPS/Galileo precise point positioning using un-differenced and between-satellite single difference measurements: Geomatica, **68**(3), 195-205.

Albayrak, M., Erdoğan, B., and Erkaya, H., 2020, Performance analysis of web-based relative and precise point positioning techniques with different satellite visibility conditions: Boletin de Ciências Geodésicas, **26**(1).

Alkan, R. M., Saka, M. H., Ozulu, İ. M., and İlçi, V., 2017, Kinematic precise point positioning using GPS and GLONASS measurements in marine environments: Measurement, **109**, 36-43.

Bahadur, B., and Nohutcu, M., 2019, Comparative analysis of MGEX products for post-processing multi-GNSS PPP: Measurement, **145**, 361-369.

Bisnath, S., and Gao, Y., 2009, Current state of precise point positioning and future prospects and limitations, in Observing our changing earth: Springer, Berlin, Heidelberg, 615-623.

Boehm, J., Werl, B., and Schuh, H., 2006, Troposphere mapping functions for GPS and very long baseline interferometry from European Centre for Medium-Range Weather Forecasts operational analysis data: J. Geophys. Res., Solid Earth, **111**(B2).

Cao, W., Hauschild, A., Steingenberger, P., Langley, R. B., Urquhart, L., Santos, M., and Montenbruck, O., 2010, Performance evaluation of integrated GPS/GIOVE precise point positioning: Proceedings of the 2010 International Technical Meeting of the Institute of Navigation, 540-552.

Dalla Torre, A., and Caporali, A., 2015, An analysis of intersystem biases for multi-GNSS positioning: GPS Solutions, **19**(2), 297-307.

Falcone, M., 2016, GALILEO System Status: Proceedings of the ION GNSS 2016, Portland, OR, USA, 2410–2430.

Jan, K., and Pierre, H., 2001, Precise point positioning using IGS orbit and clock products: GPS Solution, **5**(2), 12-28.

Li, P., and Zhang, X., 2014, Integrating GPS and GLONASS to accelerate convergence and initialization times of precise point positioning: GPS Solutions, **18**(3), 461-471.

Mendez Astudillo, J., Lau, L., Tang, Y. T., and Moore, T., 2018, Analysing the zenith tropospheric delay estimates in on-line precise point positioning (PPP) services and PPP software packages: Sensors, **18**(2), 580.

Montenbruck, O., Steigenberger, P., Khachikyan, R., Weber, G., Langley, R., Mervart, L., and Hugentobler, U., 2014, IGS-MGEX: preparing the ground for multi-constellation GNSS science: Inside GNSS, **9**(1), 42-49.

Montenbruck, O., Steigenberger, P., Prange, L., Deng, Z., Zhao, Q., Perosanz, F., Romero, I., Noll, C., Stürze, A., Weber, G. and Schmid, R., 2017. The Multi-GNSS Experiment (MGEX) of the International GNSS Service (IGS)–achievements, prospects and challenges. Advances in space research, **59**(7), pp.1671-1697.

Ogutcu, S., 2020, Assessing the contribution of Galileo to GPS+ GLONASS PPP: Towards full operational capability: Measurement, **151**, 107143.

Paziewski, J., Sieradzki, R., and Baryla, R., 2018, Multi-GNSS high-rate RTK, PPP and novel direct phase observation processing method: application to precise dynamic displacement detection: Measurement Science and Technology, **29**(3), 035002.

Rizos, C., Janssen, V., Roberts, C., and Grinter, T., 2012, Precise Point Positioning: Is the era of differential GNSS positioning drawing to an end: FIG Working Week 2012, 1-17.

Xu, G., Wang, Q., and Ma, J., 2020, OPUS-refine: a fast sampling-based framework for refining protein backbone torsion angles and global conformation: Journal of Chemical Theory and Computation, **16**(2), 1359-1366.

Yavaşoğlu, H., Tarı, E., Tüysüz, O., Çakır, Z., and Ergintav, S., 2011, Determining and modeling tectonic movements along the central part of the North Anatolian Fault (Turkey) using geodetic measurements: Journal of Geodynamics, **51**(5), 339-343.